

Chapter 2

Mechanical testing of soft tissues by indentation

In this chapter, we introduce methods to measure the mechanical properties of soft biomaterials and focus on indentation with a spherical tip. The key considerations regarding the scale, modes of operations, and mechanical models are discussed. In the end, guidelines for selecting the indentation profile, when the mechanical behavior of the sample is unknown, is given.

Keywords: Indentation models – Elastic modulus – Hertz – Oliver-Pharr – Adhesion – Stress relaxation – Creep – Dynamic Modulus – Indentation modes

This chapter is part of the doctoral thesis written by Nelda Antonovaite titled "Exploring the mechanical microenvironment of the brain by dynamic indentation".

2

2.1 Methods to measure mechanical properties

There are various mechanical testing devices available for the characterization of biological samples. Based on the geometry of the deformation, two groups can be defined: devices that measure global properties or devices that can measure local mechanical properties. Global mechanical testing devices, such as rheometer, compression, and tension devices, perform deformation of the entire sample in one of the deformation modes: compression, tension, or shear. They are suitable for homogeneous samples as they measure averaged response of the entire specimen. Local mechanical testing devices, such as atomic force microscopy (AFM), micro-, and nano-indenters, deform the sample by pushing on the surface (indenting) with a small tip, such as a sphere. Indentation can be performed at various locations over the sample to create maps of mechanical properties and, thus, indentation is suitable for heterogeneous samples. Global mechanical testing devices measure stress and strain, whereas indentation devices measure indentation-depth and applied force. Both can operate in static and dynamic modes to characterize elastic, viscoelastic, or more complex mechanical behavior.

Recently, new types of mechanical testing devices emerged where the deformation of the sample is monitored by imaging techniques from which local mechanical properties are computed. For example, in magnetic resonance elastography (MRE), the sample is placed on a vibration source to induce mechanical shear waves at a micrometer scale. Share waves travel slower in harder materials and vice versa [54], and can be monitored with phase-sensitive magnetic resonance imaging (MRI). In this way, one can produce quantitative images of wave velocities and then translate them to viscoelastic parameters. However, the resolution of MRE is limited to a few hundreds of micrometers. In ultrasound elastography (UE), on the other hand, ultrasonic transducers are used as both compression and imaging devices and can operate in both static and dynamic modes [55, 56]. Although the penetration depth of UE is at the centimeter scale, the resolution is limited to millimeters. Finally, similar to other techniques, during optical coherence elastography (OCE), deformation is induced with an actuator at a micrometer scale and monitored with optical coherence tomography (OCT). OCE can achieve a resolution of 1-100 μm but it is limited in penetration depth (from a few hundred μm to a few mm, see review [57]). The main advantage of these techniques is that they are noninvasive and, thus, can be used in clinical studies.

Most recently Brillouin microscopy (BLS) has been developed which relies on the relationship between frequency shift of incident and scattered light due to interaction between intrinsic acoustic and light waves, and longitudinal modulus in GHz frequency range [58, 59]. BLS can achieve subcellular resolution (limited by diffraction). However, penetration depths are only a few hundred microns (limited by scattering). Therefore, the technique is most suitable for single-cell studies, although it has been also applied on tissue surfaces as a non-contact mechanical testing alternative [60]. Another technique that aims to measure tissue mechanics in a non-contact manner is laser speckle microrheology (LSM) where the sample is illuminated by a coherent laser and a backscattered speckle pattern is detected in space and time. The time-varying speckle intensity is sensitive to particle displacements in the material, which depends on the viscoelastic properties of the surroundings of these particles [61]. The resolution of

2.2 Experimental considerations

LSM is at tens of micrometers while imaging depth is up to 2 mm, which together with a high-speed, large field-of-view and physiologically relevant frequency range seems to be the future technology for non-contact mechanical characterization technique for tissues.

Similar to tissues, various testing devices exist for mechanical characterization of single cells which are suitable for non-adherent or adhered cells, or both. Active techniques directly deform the cell which includes AFM, micropipette aspiration, fluid deformation cytometry, magnetic twisting cytometry, optical tweezers, parallel-plate rheometry, and optical stretching [62]. Passive techniques monitor cell-induced deformation of the substrate during traction force microscopy or particle movement inside the cell during particle tracking microrheology [63].

While new techniques are emerging, indentation on cells and tissues is still used as a golden standard for mechanical testing. Due to its low cost and relatively simple operation, the indentation remains the most popular mechanical characterization technique. Furthermore, new contact mechanics models are being developed, which increases the precision of mechanical characterization and provides new mechanical parameters. In this chapter, we will overview experimental considerations for testing soft tissues and cells by indentation.

2.2 Experimental considerations

2.2.1 Control modes of deformation

Indenter consists of a piezo-transducer and a spring, such as a cantilever, to measure the response of the material to the deformation induced by the tip (e.g. a sphere, see Fig. 2.1). Indentation-depth $d_{\text{indentation}}$ is calculated by subtracting spring deflection $x_{\text{deflection}}$ from the displacement of piezo while in contact $d_{\text{piezo-contact}}$: $d_{\text{indentation}} = d_{\text{piezo-contact}} - x_{\text{deflection}}$. The load $F(N)$ is obtained by multiplying cantilever deflection $x_{\text{deflection}}$ with a spring constant $k(N/m)$: $F = k \times x_{\text{deflection}}$. Therefore, there exists three different control modes: piezo-displacement, load, and indentation-depth.

Piezo-displacement control mode operates in an open-loop where indentation-depth and load, as well as the speed at which the indentation-depth is reached, are not controlled and depend on the relation between the spring constant of the cantilever and the stiffness of the sample. For example, in piezo-displacement mode, stiffer sample regions are measured at lower depth and lower indentation-speed compared to softer ones. Typically, the mechanical properties of biological materials stiffen with depth of indentation and indentation-speed. Therefore, measuring in piezo-displacement mode results in inaccurate comparison in that differences between soft and stiff regions are less pronounced than they actually are. Hence, the piezo-displacement mode should be only used in the linear viscoelastic regime (linear refers to a linear relationship between stress and strain, which gives depth-independent mechanical properties), which for biological materials is $\sim 1\%$ strain, and at very high or low deformation rates so that instantaneous or equilibrium time-dependent properties are measured.

Load and indentation-depth control modes operate in closed-loop, meaning that maximum indentation-depth and load, as well as the deformation rate, can be selected

2

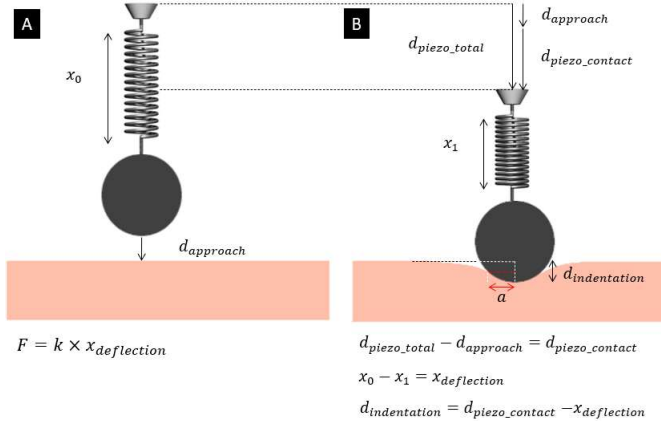


Figure 2.1: Schematic drawing of indentation. Left: the sphere is connected to a spring with an initial spring size of x_0 and distance to the sample $d_{approach}$. Right: sphere with the spring is displaced by moving it down with the piezo-transducer by a distance d_{piezo_total} , which is a sum of the distance before the contact ($d_{approach}$) and in contact ($d_{piezo_contact}$). During the deformation of the sample, the spring compresses by $x_{deflection}$. The indentation-depth $d_{indentation}$ is calculated as the difference between the piezo-displacement while in contact $d_{piezo_contact}$ and the distance of spring compression $x_{deflection}$. The load is obtained by multiplying the spring constant k by the spring compression $x_{deflection}$.

and controlled. Such an indentation approach relies on a feedback-loop where an error signal between the set profile and the actual one is calculated in real-time and used to adjust the movement of the piezoelectric transducer so that the selected indentation profile is achieved and maintained [64]. This is important for testing more complex material properties such as nonlinear viscoelasticity, where control of depth and speed is critical. Furthermore, the implementation of closed-loop operation expands possible experimental protocols to creep or stress relaxation measurements, frequency or amplitude sweeps, and oscillatory ramps.

2.2.2 The scale of mechanical testing

The first consideration before starting indentation measurements is the tip size, which will determine the mapping resolution and the indentation-depth. Spherical tips are usually selected for indentation on soft tissues to avoid damage. When spherical surface is used, stress is distributed more homogeneously compared to sharp tips. Furthermore, there is no need to align and orient the tip with respect to the sample - a problem for, for instance, flat punches. Fig. 2.2 A shows a drawing of three spherical tips on top of a brain tissue slice of 300 μm thickness, which is optimal for diffusion to ensure cell viability across the sample thickness. Indentation with the spherical tips is limited by Hertz model assumptions, described in Section 2.3.1. The finite thickness of the sample limits the maximum indentation depth d_{max} to 5% of the sample thickness,

2.2 Experimental considerations

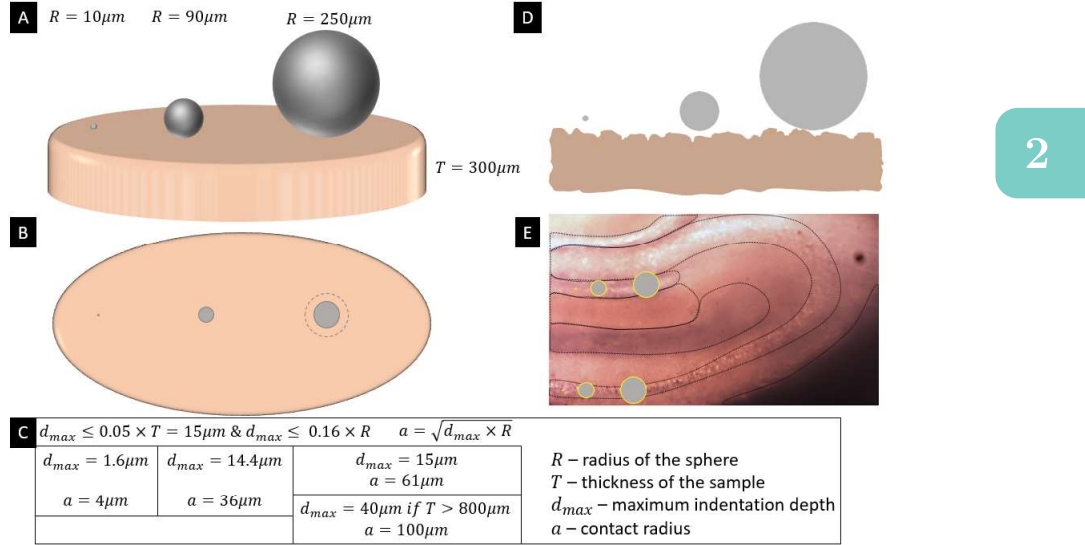


Figure 2.2: Considerations of the tip size for indentation on tissues. A) Thickness of the sample limits the maximum indentation depth to 5% of the thickness which is 15 μm . B) The contact area in gray at maximum indentation depth d_{max} = 1.4, 14.4, 15 μm for tip radius of R = 10, 90, 250 μm defines spatial resolution during indentation mapping (dashed circle for d_{max} of 40 μm if the sample thickness is over 800 μm). C) Calculation of maximum indentation depth and contact radius for three tip sizes. D) Cross-section of the slice showing the surface roughness. E) The contact area with respect to the heterogeneity of the brain tissue where boundaries of regions are identified with black lines.

which in this example is 15 μm [65]. At larger depths, the stiff substrate underneath the sample would influence the measured sample stiffness. Maximum indentation-depth is also limited to 16% of the sphere radius (small strain approximation for parabolic indenter [66]) which is $d_{max} = 1.6 \mu m$ for tip radius $R = 10 \mu m$, $d_{max} = 14.4 \mu m$ for $R = 90 \mu m$ and $d_{max} = 40 \mu m$ for $R = 250 \mu m$ where the latter is limited by finite thickness assumption $d_{max} = 15 \mu m$ and would require a sample thickness of 800 μm to indent up to 40 μm . Therefore, smaller tips measure surface properties while larger tips can indent deeper and, thus, obtain more bulk properties. However, if the surface of the sample is rough as shown in Fig. 2.2 E on the image of the hippocampus, a small sphere can easily measure the narrowest regions, while a large sphere would also sense the surrounding regions. Here, the contact radius is given for the maximum indentation depth d_{max} and, one could decrease the indentation-depth to decrease

The tip size and maximum indentation depth defines the spatial resolution which can be calculated from contact radius $a = \sqrt{d_{max}R}$ which is 4, 36 and 61 μm , respectively (see Fig. 2.2 B). The spatial resolution which is a step size during indentation mapping should be smaller than the dimensions of regions of interest to fulfill the infinite half-space assumption. As shown in Fig. 2.2 E on the image of the hippocampus, a small sphere can easily measure the narrowest regions, while a large sphere would also sense the surrounding regions. Here, the contact radius is given for the maximum indentation depth d_{max} and, one could decrease the indentation-depth to decrease

the contact radius. Therefore, optimal tip radius and indentation-depth need to be selected based on the size of the region under investigation.

2

The same considerations can be applied for measuring single cells. As cells are relatively thin, indentation-depth is of extreme importance to avoid sensing the substrate, which would cause an overestimation of stiffness. However, if the measuring system has a relatively high noise level and only large indentation depths can be resolved, the correction of modulus because of the stiff substrate and large indentation depths can be applied [67, 68]. However, such a correction requires additional measurements of the cell thickness. Furthermore, cells vary in shapes for which corrections of the Hertz model exist to account for hemispherical or spherical shapes [69]. This can be avoided by selecting a smaller tip size so that the measured location can be considered flat compared to the tip size. However, small tip size limits maximum indentation-depth, which might be of relevance when studying membrane versus cytoskeleton properties. Finally, measuring the nuclear or cytoskeleton part of the cell should be discriminated, as these two sub-cellular structures have differential mechanical properties. Especially when measuring the cell nucleus of an intact cell, the influence of the cytoskeleton above and below the nucleus should be acknowledged.

To summarize, mechanical characterization by indentation requires careful consideration of the relevant measurement scale while also fulfilling the contact mechanics model assumptions.

2.3 Contact mechanics models for indentation

2.3.1 Static indentation models

During static indentation, the tip of the indentation probe is forced onto the sample and retracted (Fig. 2.3 A). These two static indentation steps are commonly called loading and unloading. Static indentation is used to measure the elasticity of elastic or elastic-plastic materials in terms of hardness or Young's modulus. In particular, this section discusses Hertz, Oliver-Pharr, and JKR model solutions for spherical tips.

The Hertz model

The Hertz model was derived by Heinrich Hertz in 1882 [70] and gives an analytical solution of the non-adhesive contact problem between elastic materials. Based on this derivation, a simple solution was given to estimate the contact radius a (red dashed line in Fig. 2.1 B) when indenting with a sphere on an infinite elastic half-space:

$$a = \left(\frac{3FR}{4E_{eff}} \right)^{1/3}, \quad (2.1)$$

where F is the applied load, R is the radius of the spherical indenter, and E_{eff} is the effective elastic modulus also referred as plain strain or reduced or apparent Young's modulus. Moreover, the relation between the indentation-depth h_c and the contact

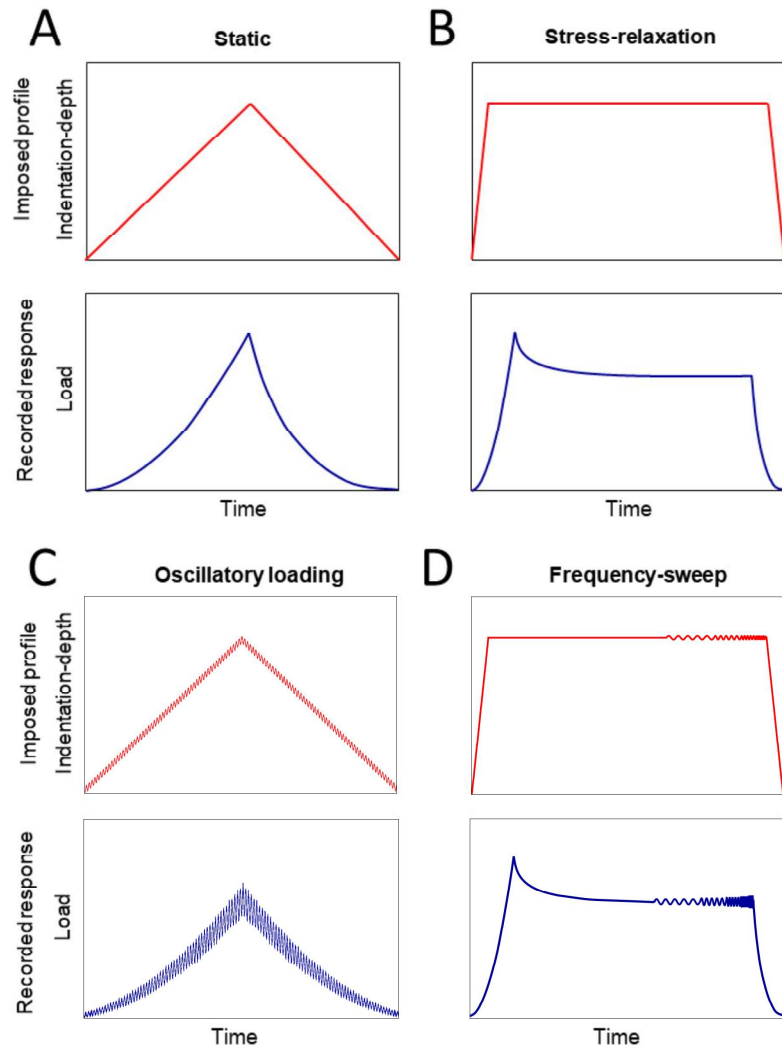


Figure 2.3: Imposed indentation-depth controlled profiles in red and recorded load response in blue. A) Static indentation with no holding phase; B) static indentation with holding phase for stress-relaxation; C) dynamic indentation with oscillatory loading and unloading; D) dynamic indentation with frequency sweep at equilibrium.

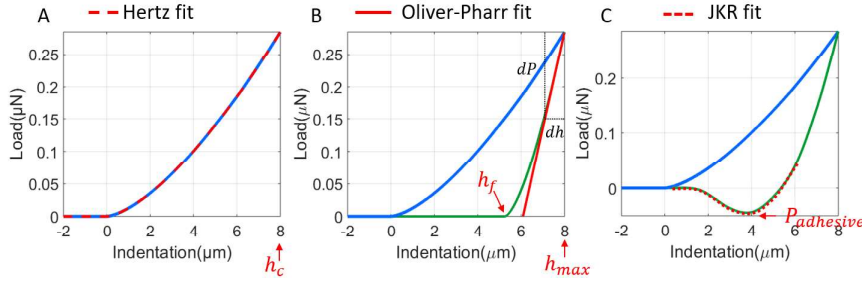


Figure 2.4: Load-indentation curves of A) loading (blue line) with Hertz model fit (dashed red line) for elastic materials; B) loading (blue line) and unloading (green line) with Oliver-Pharr model fit (red line) for elastic-plastic materials; C) JKR model fit (dashed red line) for elastic-adhesive materials.

radius a can be defined from the geometry of the system as:

$$h_c = \frac{a^2}{R}. \quad (2.2)$$

This definition relies on a parabolic approximation of the shape of the indenter, meaning it is only valid when $h_c \ll R$. More recently, equation 2.2 was shown to hold for strains less than 8% [66], resulting in maximum indentation depth $h_c = 16\% \times R$.

By substituting contact radius a from equation 2.1 into equation 2.2, the relationship between load and indentation can be defined and used to fit initial load-indentation curve (see Fig. 2.4 A):

$$P = \frac{4}{3} E_{eff} R^{1/2} h_c^{3/2}, \quad (2.3)$$

the effective Young's modulus combines the response of the sample and indenter and depends on the Poisson ratio:

$$\frac{1}{E_{eff}} = \frac{1 - \nu_1^2}{E_1} + \frac{1 - \nu_2^2}{E_2}. \quad (2.4)$$

Assuming that the indenter is much stiffer than the tested material, the Young's modulus of the material can be approximated by:

$$E = \frac{E_{eff}}{1 - \nu^2}. \quad (2.5)$$

where ν is the Poisson's ratio of the indented material. Biological tissues are typically assumed to be incompressible with $\nu = 0.5$.

The derivation of the Hertz model relies on several assumptions:

1. The deformation is linear elastic;
2. Strains are small that the indenter can be assumed to be parabolic;
3. The thickness and size of the sample are infinite in relation to the tip size;

2.3 Contact mechanics models for indentation

4. The sample is homogeneous and isotropic;
5. The surface of the sample is flat in relation to the tip size;
6. The surfaces are frictionless and non-adhesive;
7. The tip and measurement system are infinitely stiff compared to the stiffness of the sample;

As other contact mechanics models described in the following sections are based on Hertz model assumptions, careful assessment of their validity for each experiment is required. In case some assumptions are not fulfilled, the influence to elastic modulus estimation should be addressed. For example, the Hertz model is widely used to obtain the elastic modulus of viscoelastic materials, which, for comparative analysis with a carefully selected indentation profile, can be accepted.

The Oliver-Pharr model

Warren Oliver and George Pharr published the derivation of the elastic modulus of elastic-plastic materials from load-indentation curves in 1992 [71], which was later adapted to include indentation with a spherical tip [72]. Indentation of elastic-plastic material results in mismatched loading and unloading curves because of a dent left after the load is removed. In this case, the contact area A between the tip and the sample must be correctly modeled. The contact depth (h_c) of the sphere can be determined from the final and maximum indentation depths (h_f and h_{max} , respectively, see Fig. 2.4 B):

$$h_c = h_{max} - h_f \quad (2.6)$$

The final indentation depth h_f is the depth where, during unloading, the load equals zero. From a geometrical point of view, contact radius a can be calculated from:

$$a = \sqrt{(2Rh_c - h_c^2)}, \quad (2.7)$$

The quadratic term becomes negligible when indentation depth h_c is much smaller than the radius R of the indenter. Assuming initial elastic unloading, the Young's Modulus E of the indented material can be estimated:

$$E = \frac{S\sqrt{\pi}}{2\sqrt{A}}(1 - \nu^2). \quad (2.8)$$

Here, $S = dP/dh$ is the slope of the initial unloading curve (i.e., 95% and 75% of the load at the maximum indentation, see Fig. 2.4 B) and $A = \pi a^2$ is the contact area.

The same Hertz model assumptions hold for the Oliver-Pharr model. The Oliver-Pharr model has been widely used to calculate the elastic modulus of biological materials that are not elastic-plastic but viscoelastic. This might give misleading results, especially when using a short holding time between loading and unloading as viscoelastic material relaxes over time. How to use elastic and elastic-plastic models for viscoelastic materials will be discussed in Section 2.3.1.

JKR model

Adhesion is attachment or attraction between the tip and the sample and it is not included in Hertz contact mechanics model. However, it has been widely studied by others [73–77]. The effects of adhesion include an increase in contact area a during indentation and negative loads during unloading (i.e. the sample adheres to the tip). Analytical models such as the JKR [73] and the DMT models [74] provide modified Hertz equations with adhesion taken into account. The JKR model is developed for a large tip radius R when indenting on soft materials, whereas the DMT model predicts the indentation behavior of a stiff material probed with a small tip radius. The separation between the two models was given by Tabor [75], who introduced a coefficient μ :

$$\mu = \left(\frac{R\gamma^2}{E_{eff}^2 z_0^3} \right)^{\frac{1}{3}}, \quad (2.9)$$

where z_0 is the equilibrium separation between the atoms of the surfaces in contact (i.e., the distance between the atoms at which the force on each atom is zero) and γ is the energy per unit contact area, also termed as “work of adhesion”, which depends on the surface energies of the two contacting surfaces and an interaction term ($\gamma = \gamma_1 + \gamma_2 - \gamma_{12}$). If μ is large, JKR theory applies; and if it is small, the DMT model applies. The DMT model is not further discussed, as its applications lie beyond the scope of this thesis. Following the JKR model, a description of γ can be obtained based on the critical load $P_{adhesive}$ at which the indenter separates from the surface (i.e. the maximum adhesive force, as illustrated in Fig. 2.4 C):

$$\gamma = -\frac{3}{2} \frac{P_{adhesive}}{\pi R}. \quad (2.10)$$

The contact radius at a given load P is modified from the Hertz equation to include the contact surface energy γ :

$$a^3 = \frac{3R}{4E_{eff}} \left(P + 3\gamma\pi R + \sqrt{6\gamma\pi RP + (3\gamma\pi R)^2} \right). \quad (2.11)$$

When $\gamma = 0$ equation 2.11 reverts to the simple Hertz equation without adhesion. However, in case of adhesion ($\gamma \neq 0$), at $P = 0$ the contact radius becomes non-zero and is given by:

$$a_0^3 = \frac{18\gamma\pi R^2}{4E_{eff}} \quad (2.12)$$

and the indentation depth can be estimated as:

$$\delta = \frac{a^2}{R} \left(1 - \frac{2}{3} \left(\frac{a_0}{a} \right)^{\frac{3}{2}} \right). \quad (2.13)$$

Using this modified description of the contact radius a , a correct value for the effective Young's modulus E_{eff} can be computed by fitting the unloading curve (see Fig. 2.4 C) while fulfilling all the other Hertz model assumptions.

In the case of indenting on adhesive viscoelastic materials, novel contact mechanics

2.3 Contact mechanics models for indentation

models have been proposed to account for adhesion when calculating time or frequency-dependent elastic modulus [77, 78]. However, as these models are more computationally and in some cases experimentally demanding, they have not yet been widely adapted and adhesion has been often neglected on the basis that the nominal forces dominate over adhesive forces.

Static indentation for viscoelastic materials

In many studies, static indentations and elastic mechanical models, such as Hertz and Oliver-Pharr, are used to characterize viscoelastic materials, including soft tissues and cells, due to a lack of more advanced instrumentation, easy data analysis, and because it has been done in previous studies. In this section, recommendations on how to make the most use of static indentations for the characterization of viscoelastic materials will be given.

Static indentation enables measurements of hundreds of indentation locations in a very short time. As biological samples quickly deteriorate when taken out of an incubator or extracted from an animal or human, static indentations might be preferred over slow dynamic measurements (more details in Section 2.3.2). Data from single static indentations with only loading and unloading phases can be analyzed with the elastic Hertz contact mechanics model. Elastic material properties are time-independent, i.e. loading and unloading rates do not influence the measured elastic modulus. However, that is not the case for viscoelastic materials where the elastic modulus is time-dependent. Typically, the faster the indentation the higher the elastic modulus. Furthermore, load-indentation curves of viscoelastic materials exhibit hysteresis between loading and unloading phases, which might be mistaken for plastic deformation and, thus, analyzed by the elastic-plastic Oliver-Pharr model. While, in principle, elastic and elastic-plastic models are not suitable for the characterization of viscoelastic materials, it might give sensible results if time dependency is considered. For example, indenting at high indentation-speed gives Young's modulus similar to instantaneous modulus when considering time-domain or modulus at high frequencies when considering frequency domain [79]. Alternatively, measuring at low indentation rates gives properties similar to equilibrium modulus or low-frequency modulus. Thereby, using the Hertz model, relative comparisons can be made if the same indentation-speed is used (note: indentation speed is not the same as piezo-speed). For the Oliver-Pharr model, the unloading curve used for fitting is influenced by the loading history, which should therefore be taken into account, e.g. by using a long holding phase to reach equilibrium before unloading [80, 81]. Finally, by combining results from static measurements at different indentation rates with solutions from computation analysis, viscoelastic parameters can also be extracted [82, 83].

2.3.2 Dynamic indentation models

In the previous section, we discussed how static indentation measurements, consisting of loading and unloading phases, have been used to obtain the elastic modulus of

biological materials. However, Young's modulus dependency on indentation rates is a clear sign of viscoelasticity. Here, we will overview time-dependent indentation measurements, i.e., dynamic indentation.

2

Time domain: creep and stress relaxation

A frequently used method to investigate linear viscoelastic behavior by indentation is to apply constant stress via a step-function and monitor the increase in strain over time, which is called creep. During the indentation test, stress and strain are not measured directly and, thus, stress can be approximated with the applied load and the strain with the indentation-depth.

A simple model that is often used to simulate the creep behavior is the Kelvin-Voigt model. It consists of a spring and dashpot connected in parallel and may be expanded by adding more springs and dashpots. The indentation-depth response of this system over time $h(t)$ to a constant applied load P is given by creep function $J(t)$:

$$h(t)^{3/2} = \frac{3}{8} \frac{P}{\sqrt{R}} J(t). \quad (2.14)$$

$$J(t) = C_0 - \sum_i C_i e^{-t/\tau_i}. \quad (2.15)$$

where τ_i are time constants of creep, C_i are creep coefficients, from which the zero-time (instantaneous) shear modulus can be calculated as $G_0 = \frac{1}{2(C_0 - \sum_i C_i)}$ and the infinite-time shear modulus as $G_\infty = \frac{1}{2C_0}$ [84, 85]. The shear modulus is then related to Young's modulus through Poisson's ratio: $E = 2G(1 + \nu)$.

To maintain constant stress during creep experiments, a load-controlled indentation is required. During the creep, indentation-depth, strain, and contact area changes. One needs to keep in mind that the increase in indentation-depth may exceed the linear regime where mechanical properties are depth-independent. In a non-linear regime, it may be more practical to use a stress relaxation method.

During stress relaxation experiments, indentation-depth is kept constant and the decrease in load over time is monitored (Fig. 2.3 B). Stress relaxation of linear viscoelastic materials is modeled by a Maxwell model, which consists of a spring and dashpot placed in series. Shear modulus can be calculated with Boltzmann hereditary integral [86, 87]:

$$P(t) = \frac{8}{3} \sqrt{R} h_c^{3/2} G(t). \quad (2.16)$$

where h_c is the indentation depth and $G(t)$ can be fit with Prony series:

$$G(t) = C_0 + \sum_j C_j e^{-t/\tau_j}. \quad (2.17)$$

where τ_j are time constants of exponential decay and C_j are relaxation coefficients. The instantaneous modulus G_0 can be calculated with equation $G_0 = C_0 + \sum_j C_j$ and the equilibrium (infinity) shear modulus is $G_\infty = \frac{C_0}{2}$.

Via a multi-exponential fit applied to creep or relaxation data from the holding

2.3 Contact mechanics models for indentation

phase, one can estimate the shear moduli G_t at different time points, besides instantaneous and infinity moduli. However, creep and stress relaxation curves from biological materials typically require 3 or more-term exponential fits, while the data also has a low signal-to-noise ratio, leading to results that strongly depend on the fitting initial parameters.

It is worth stressing that, to translate shear moduli from time to frequency domains, one can use the following equations:

$$G'(\omega) = G_\infty + \sum_{j=1} G_j \frac{(\omega\tau)^2}{1 + (\omega\tau)^2}. \quad (2.18)$$

$$G''(\omega) = G_\infty + \sum_{j=1} G_j \frac{\omega\tau}{1 + (\omega\tau)^2}. \quad (2.19)$$

or, vice versa:

$$G(t) = \int_0^\infty \frac{G'(\omega)}{\omega} \sin(\omega t) dx \quad (2.20)$$

where data needs to be extrapolated to zero and infinite frequencies [88].

Dynamic mechanical analysis (DMA)

As an alternative to the approach described above, indentation measurements can be performed in the frequency domain to obtain storage and loss moduli as a function of frequency.

Dynamic mechanical analysis (DMA) is based on inducing oscillations of the load (or indentation-depth) at different frequencies (frequency sweep), on top of a feedback-controlled constant load (or indentation-depth) (Fig. 2.3 D). The storage modulus E' represents the capacity to store energy because of the elastic component; the response is in-phase with the applied load. The loss modulus E'' represents the capacity to dissipate energy due to the viscous component; the response is out-of-phase with the applied load. The ratio $E''/E' = \tan \phi$ is the damping factor or loss angle, and shows the relative degree of how well a material can dissipate or, in other words, absorb energy [89].

This approach was developed by Herbert, Oliver, and Pharr [89], who related stress and strain to load and indentation. For a spherical indenter, the storage and loss moduli can be calculated from the load and indentation signals for each oscillation frequency ω :

$$E'(\omega) = \frac{P_0}{h_0} \cos(\phi) \frac{1 - \nu^2}{a} \quad (2.21)$$

and

$$E''(\omega) = \frac{P_0}{h_0} \sin(\phi) \frac{1 - \nu^2}{a}, \quad (2.22)$$

with ϕ being the phase difference between oscillations, P_0 the amplitude of the oscillatory load, h_0 the amplitude of the oscillatory indentation-depth, and a the

radius of the contact area. For purely elastic Hookean solids, phase shift ϕ is 0° while for Newtonian liquids the phase-shift is 90° . For viscoelastic-liquids, the phase-shift is between 45 and 90° ($\tan\phi > 1$), while for viscoelastic-solids, it is between 0° and 45° ($0 < \tan\phi < 1$) which is usually the case for cells and tissues.

2

Complex modulus sums up the storage and loss moduli:

$$|E^*| = \sqrt{E'^2 + E''^2}. \quad (2.23)$$

Complex dynamic viscosity can be calculated as follows:

$$|\eta^*| = \frac{E^*}{\omega}. \quad (2.24)$$

To avoid the influence of creep or stress-relaxation to oscillatory signal, the frequency sweep is recommended to be performed after the equilibrium is reached as shown in (Fig. 2.3 D). Furthermore, one can also apply oscillations at one frequency during the loading phase (Fig. 2.3 C) by selecting a slow loading rate so that the material is at equilibrium while loading (more details in Chapter 3, Section 3.3.2). Moreover, the amplitude of oscillations should be small enough to fulfill the approximation of constant contact area during oscillations which depends on indentation-depth and tip radius. For instance, oscillating at $0.1 \mu\text{m}$ amplitude with tip radius of $10 \mu\text{m}$ at $1 \mu\text{m}$ indentation-depth would result in $0.32 \mu\text{m}$ change of contact radius Δa , while oscillating at $0.5 \mu\text{m}$ amplitude, the contact radius would change $1.64 \mu\text{m}$. To assess whether the amplitude of oscillations influences the measurement, one can check the symmetry of the oscillations. Based on experimental observations, we recommend using these criteria: $\frac{\Delta a}{a} < 0.1 \mu\text{m}$ (more details in Chapter 3, Section 3.3.3).

Combining all the previous approaches, one could perform a Hertz model fit, creep or stress relaxation analysis, dynamic mechanical analysis, the Oliver-Pharr model fit, and even an adhesion analysis from one indentation curve. Practically, however, one should select the preferred method for the sample under investigation and optimize the indentation profile so that all assumptions are satisfied.

Depth-dependency: linear and nonlinear regimes

The deformation of material can have two regimes: linear and nonlinear. During the linear regime, stress and strain scale linearly, whereas beyond the limit of the linear regime, stress and strain scaling is nonlinear. This means that at the linear regime, mechanical properties are depth independent and in the nonlinear regime, they are depth-dependent. As indentation does not give a direct measure of stress and strain, these regimes can be evaluated by applying mechanical models to different depths.

Using the Hertz model, linearity can be assessed by fitting the same load-indentation curve to different depths. If the material is nonlinear, fitting to higher depths will result in higher Young's modulus compared to fitting to lower depths, or vice versa. Furthermore, the fitting will be poor as scaling between load and indentation of nonlinear materials does not follow the $P \sim h^{\frac{3}{2}}$ relationship.

Using the Oliver-Pharr model to investigate nonlinearity, indentation needs to be performed to different depths as only the initial unloading curve is used for fitting.

2.4 Guidelines to selecting indentation profile

Due to irreversible plastic deformation, multiple indentations can not be performed in the same location, because the first indentation alters the material properties. Therefore, indentations at different depths should be performed at different locations of the sample, assuming the sample is homogeneous. It is important to note that if the Oliver-Pharr model is used for viscoelastic material, enough time for viscoelastic recovery should be given between consecutive indentations (read more in Section 2.4.3).

Previously introduced time and frequency domain contact mechanics models assume linear viscoelastic response of the material. Using dynamic methods, linear and nonlinear regimes can be assessed by performing dynamic measurements at different depths. As the analysis of DMA or stress relaxation is performed at a constant indentation-depth, actual fitting is not affected by nonlinearity.

Note: poro-viscoelasticity

Time-dependent behavior arises not only from viscoelasticity but also from poroelasticity. Viscoelastic relaxation originates from configuration change of the network, which is a short-range motion. Poroelastic relaxation arises from the migration of solvent through the pores, which is a long-range motion. However, discrimination between these two modes requires stress relaxation tests with different sphere sizes, because the poroelastic response is size-dependent while viscoelastic is size independent [90, 91]. At large length scales, poroelastic relaxation is slower than viscoelastic, while at lower length scales it is the opposite.

For the purpose of relative comparison between different samples, one can be sufficed by viscoelastic characterization, as it does not require testing with different radius probes at long time scales. However, for creating mechanical models of materials and simulating mechanical deformation, poro-viscoelastic modeling is in principle required to increase the accuracy of predictions, especially when exploring different scales.

2.4 Guidelines to selecting indentation profile

To start the mechanical characterization of a biological sample, one needs to select an appropriate indentation profile depending on the mechanical behavior such as elastic, plastic, or viscoelastic, and linear vs. nonlinear. We suggest a simple indentation procedure to determine the mechanical behavior of a material. The proposed indentation profiles are in indentation-depth controlled mode as it ensures higher accuracy over indentation-speed and indentation-depth.

2.4.1 Discrimination between elastic and viscoelastic material

Discrimination between elastic and viscoelastic material can be done either in static or dynamic modes (see Fig. 2.5), as both of methods lead to the same conclusions. We recommend using dynamic mode as it requires only one indentation, while static mode requires the use of two indentations and, thus, the same location of the sample has to

be measured twice (more details about the situations where this can be a problem are in the Section 2.4.3).

2

Static indentation-depth controlled mode

In order to determine whether the sample is elastic or viscoelastic with static indentation-depth controlled mode, the indentation should be performed at two different indentation-speeds (e.g., $v_1 = 1 \mu\text{m/s}$, $v_2 = 15 \mu\text{m/s}$), (see Fig. 2.5 top half). The initial loading part should be followed by a hold period (e.g. $t(\text{hold}) = 20 \text{ s}$). Indentation depth should fulfill small strain (ϵ) approximation $\epsilon < 0.08$, where $\epsilon = 0.2 * \sqrt{(d * R) / R}$, d is indentation depth, and R is the radius of the sphere.

If the material is elastic, the load is constant during the hold period $P_{\text{rel}} = \text{const}$ and the Young's modulus obtained from the Hertz or Oliver-Pharr models will be the same at both measured speeds: $E_{H(v1)} = E_{H(v2)}$, $E_{OP(v1)} = E_{OP(v2)}$.

If both assumptions above are correct, one can determine if the sample is purely elastic or elastic-plastic. If the sample is purely elastic, there is no hysteresis, meaning that loading and unloading curves coincide, and both Young's modulus from the Hertz model and Oliver-Pharr model are equal $E_H = E_{OP}$. If the sample behaves as an elastic-plastic material, there is hysteresis between loading (blue line) and unloading (green line), and the Young's modulus obtained with the Hertz model will be smaller than with the Oliver-Pharr model $E_H < E_{OP}$. This is in part because the Hertz model overestimates the contact area, whereas in the Oliver-Pharr model d_p (contact point during unloading) is subtracted from d_0 (contact point during loading) for the calculation of the contact area. Indeed, the Oliver-Pharr model accounts for plastic deformation.

Using the static mode, the material is considered being viscoelastic when the load decreases during the hold period (see *relaxation*). Furthermore, Young's modulus obtained from Hertz or Oliver-Pharr models will be different when comparing two measured speeds: $E_{H(v1)} < E_{H(v2)}$ or $E_{OP(v1)} < E_{OP(v2)}$. In this case, it is not possible to determine whether there is permanent plastic deformation as hysteresis between loading and unloading are due to viscoelasticity.

Dynamic indentation-depth controlled mode

Whether the sample is elastic or viscoelastic can also be determined in dynamic mode (Fig. 2.5 bottom half). A dynamic indentation consists of loading, holding period (e.g. $t(\text{hold})=20 \text{ s}$, use holding time sufficient to reach the equilibrium of relaxation), frequency sweep (e.g. 1-10 Hz), and unloading. Loading should be fast (e.g. $v_1 = 15 \mu\text{m/s}$) to observe full load-relaxation profile. In the case of slow loading, the material relaxes during the loading phase and, thus, relaxation in the holding period might be diminished. The oscillation amplitude should be small enough so that the assumption of constant contact area is valid. A good indication is checking whether oscillations are sine-shape and symmetrical. Furthermore, the selected amplitude A_ω of oscillatory indentations at different frequencies should be the same. If the amplitude is not constant or does not reach the set amount, it means that the gain, integral, and

2.4 Guidelines to selecting indentation profile

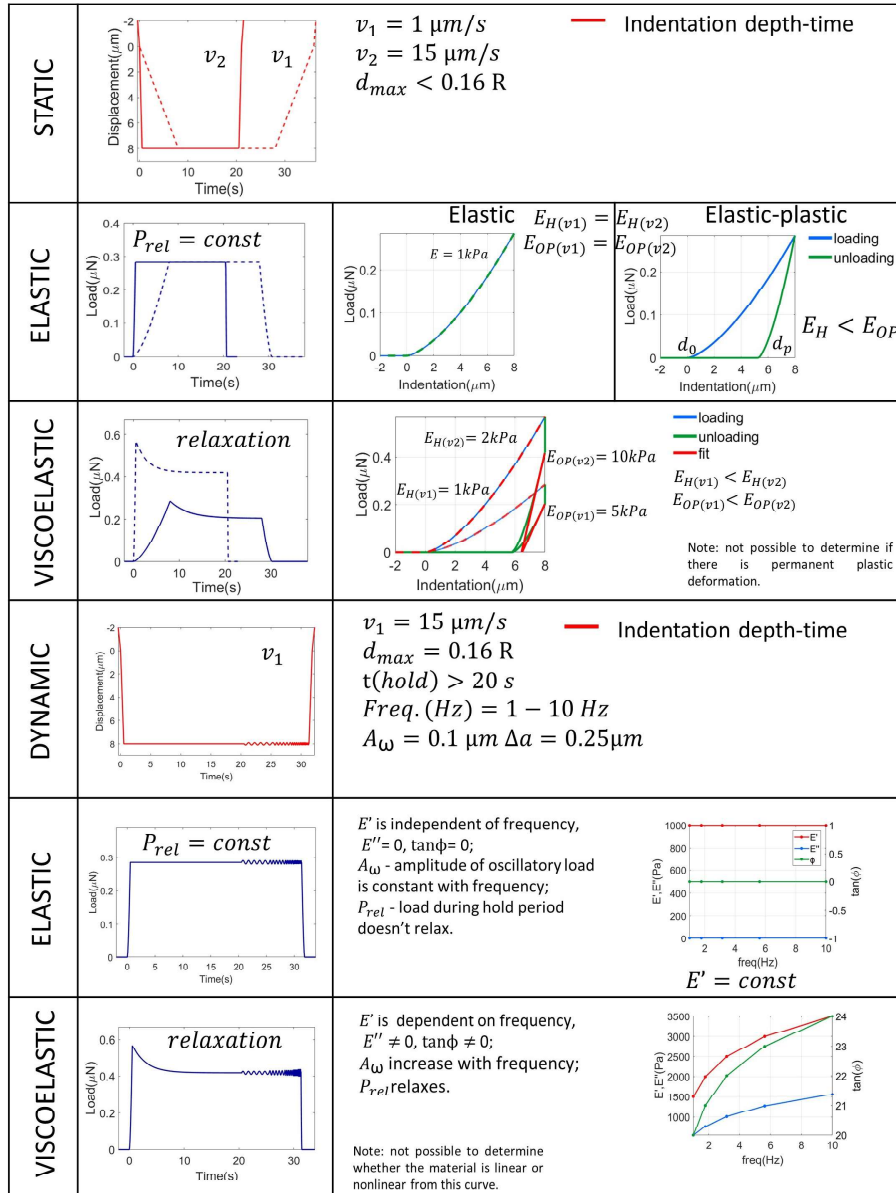


Figure 2.5: Guidelines to determine whether the material is elastic or viscoelastic using static or dynamic indentation-depth controlled profiles.

derivative (PID) settings of the feedback-loop need tuning or that the limit of the speed of the hardware and software is reached. In this case, one should either decrease the amplitude, use a stiffer probe, or decrease the frequency.

2

If the material is elastic, there is no load-relaxation during the hold period $P_{rel} = const$, storage modulus E' does not depend on frequency $E'(\omega) = const$ (constant amplitude of oscillatory load), and both loss modulus and phase delay are equal to zero ($E''(\omega) = 0$, $\phi(\omega) = 0$). Furthermore, loading data can be used to determine whether the sample is elastic or elastic-plastic as described previously.

If the material is viscoelastic, there is load-relaxation during the hold period (see *relaxation*), storage modulus E' increases with frequency, which can also be observed as an increase in the amplitude of oscillatory load, and both loss modulus and phase delay have non-zero values ($E' \neq 0$, $\phi \neq 0$).

2.4.2 Discrimination between linear and nonlinear material

Static indentation-depth controlled mode

If the sample is elastic or elastic-plastic, loading data can be used to determine whether the sample is linear or nonlinear at the measurement scale by fitting the Hertz model to different indentation-depths (see Fig. 2.6 top half). A single indentation to a larger depth (e.g., $d_2 = 8 \mu\text{m}$) is sufficient for Hertz model analysis. If the material is linearly elastic, fitting Hertz-model to different depths results in the same Young's moduli $E_{H(d1)} = E_{H(d2)}$. If the material is nonlinear elastic, fitting the Hertz model to different depths results in different Young's modulus $E_{H(d1)} \neq E_{H(d2)}$. Typically, an increase in Young's modulus with the depth is observed ($E_{H(d1)} < E_{H(d2)}$).

One could also use the Oliver-Pharr model to come to the same conclusions, but this approach requires two indentation measurements performed at two different depths (e.g., $d_1 = 4 \mu\text{m}$ and $d_2 = 8 \mu\text{m}$). If the material is elastic-plastic, indentation induces plastic deformation; thus, indentation at two different depths should be performed at different locations. If the material is linear elastic-plastic, fitting unloading data from measurements at two depths with the Oliver-Pharr model results in the same Young's modulus $E_{OP(d1)} = E_{OP(d2)}$. If the material is nonlinear elastic-plastic, the Young's modulus obtained with Oliver-Pharr model depends on the depth $E_{OP(d1)} \neq E_{OP(d2)}$. Typically, an increase in Young's modulus with the depth is observed ($E_{OP(d1)} < E_{OP(d2)}$).

Dynamic indentation-depth controlled mode

If the material is viscoelastic, to check whether the material is linear or nonlinear at the measurement scale, one should perform indentations in a dynamic mode at two different depths (e.g., $d_1 = 4 \mu\text{m}$ and $d_2 = 8 \mu\text{m}$) (see Fig. 2.6 bottom half). Sufficient time for viscoelastic recovery should be taken between repeated measurements in the same location to avoid conditioning (see section 2.4.3).

If the material is linear viscoelastic, E' , E'' , and ϕ are independent on the depth, $E'_{d1} = E'_{d2}$ at any frequency, the ratio between P_{max} and P_{min} is the same at both

2.4 Guidelines to selecting indentation profile

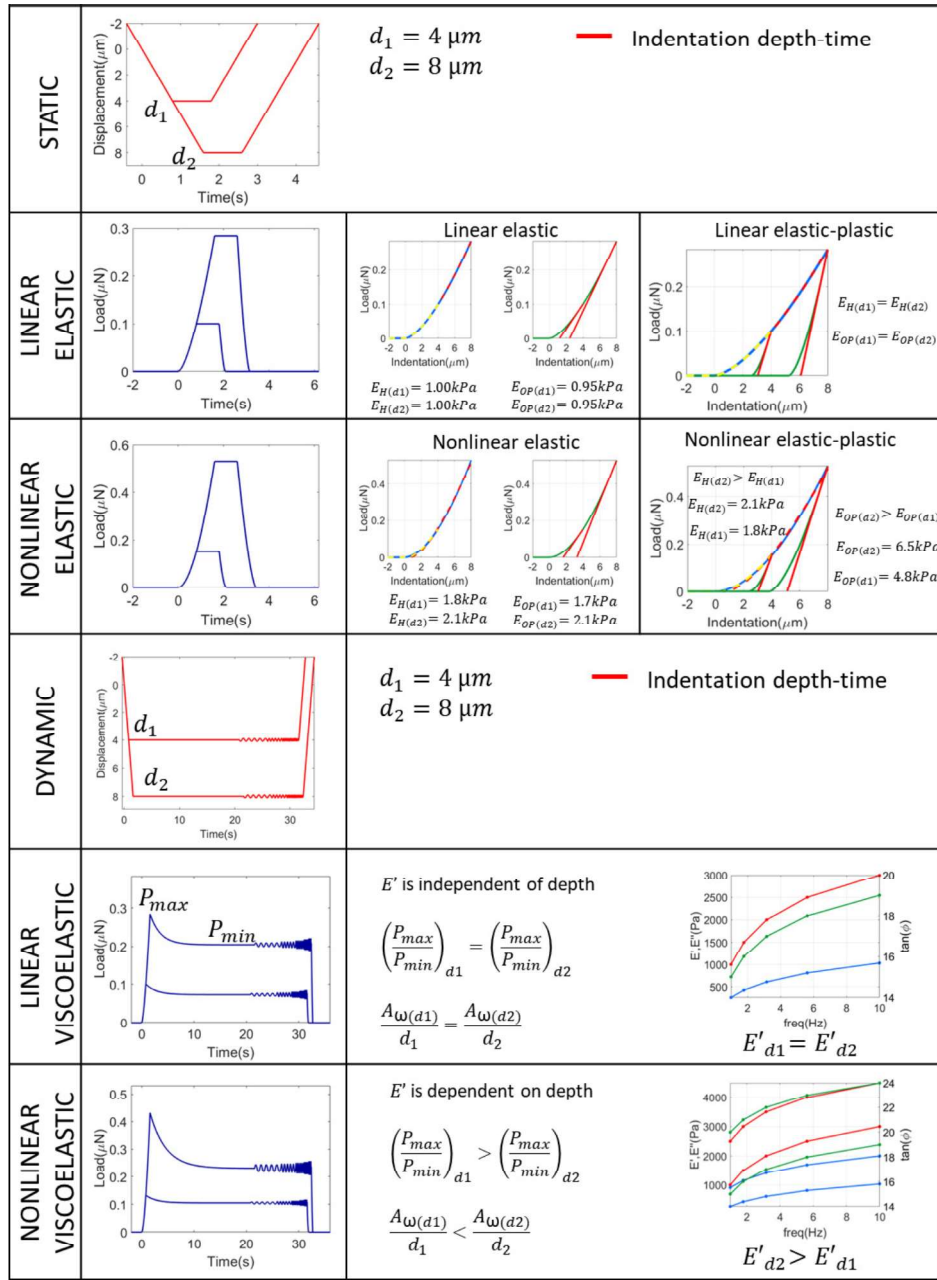


Figure 2.6: Guidelines to determine whether material is linear or nonlinear elastic or viscoelastic using static or dynamic indentation-depth controlled profiles.

depths $(\frac{P_{max}}{P_{min}})d_1 = (\frac{P_{max}}{P_{min}})d_2$, and the ratio between the amplitude of oscillatory load A_ω and indentation-depth d is the same at both depths $\frac{A_{\omega(d1)}}{d_1} = \frac{A_{\omega(d2)}}{d_2}$.

If the material is nonlinear viscoelastic, E' , E'' , and ϕ are dependent on the depth at any frequency, typically $E'_{d1} < E'_{d2}$, the ratio between P_{max} and P_{min} is different, typically $(\frac{P_{max}}{P_{min}})d_1 > (\frac{P_{max}}{P_{min}})d_2$, and the ratio between the amplitude of oscillatory-load and indentation-depth is different, typically $\frac{A_{\omega(d1)}}{d_1} < \frac{A_{\omega(d2)}}{d_2}$.

2.4.3 Conditioning

When investigating the most suitable indentation protocol, multiple indentations in the same location are required. The first indentation on the sample is called un-conditioned or virgin, while all the following indentations in the same location are called conditioned or pre-conditioned. Mechanical properties might change with each consequent indentation either due to irreversible plastic deformation or due to reversible deformation caused by visco- and poro-elasticity (time-dependent effects).

In the case of viscoelasticity, indentation induces temporary plastic deformation due to time-dependent movement of fluids and reversible rearrangement of material components. Sufficient time should be given between consequent indentations in the same location in order to allow material to recover to the original condition (read more in Chapter 3, Section 3.3.5). The time needed for the viscoelastic recovery can be assessed by performing consequent indentations with different time intervals between indentations until the time interval is found where consequent indentation gives the same mechanical properties. One should keep in mind that different indentation profiles will have different time intervals of full viscoelastic recovery. Furthermore, it might be that the material does not recover to the original condition due to irreversible plastic deformation or because the recovery time is too long in actual experimental conditions. In this case, only a single indentation should be performed per location.